**IMECE 2002:**
**2002 ASME International Mechanical Engineering Congress**
**November 17-22, 2002**

# IMECE2002-33920

# EFFECTS OF GAS RADIATION ON THE THERMAL CHARACTERISTICS OF REGENERATIVELY COOLED ROCKET ENGINES

Mohammad H.N. Naraghi  Edmundo M. Nunes

Department of Mechanical Engineering, Manhattan College, Riverdale, NY 10471

## ABSTRACT

This paper studies the effects of radiative heat transfer on the thermal characteristics of regeneratively cooled rocket engines. A conjugated radiative, conductive and convective model is used to analyze the effects of radiative heat transfer in two regeneratively cooled rocket engines. One engine has liquid hydrogen and liquid oxygen as the propellant and liquid hydrogen as the coolant. The other engine has RP1 (a hydrocarbon fuel) and liquid oxygen as the propellant and liquid oxygen as the coolant. It is shown that gas radiation has some effect on the wall temperature of the $LH_2$-$LO_2$ engine and a small effect on its coolant flow characteristics. For the RP1-LO2 engine, however, gas radiation significantly increases the coolant pressure drop, temperature and Mach number. It is also shown that radiation effects must be addressed in cooling channel design, so that wall temperatures and cryogenic coolant flow temperature/pressure are at suitable levels.

## NOMENCLATURE

| | |
|---|---|
| $C_p$ | constant-pressure specific heat |
| $dr$ | radial thickness of gas/volume ring element |
| $ds$ | width of surface ring element |
| $\overline{dgg}(\mathbf{r}_i, \mathbf{r}_j)$ | direct exchange factor between gas/volume ring elements $i$ and $j$ |
| $\overline{dgs}(\mathbf{r}_i, \mathbf{r}_j)$ | direct exchange factor between gas/volume ring element $i$ and surface ring element $j$ |
| $\overline{dsg}(\mathbf{r}_i, \mathbf{r}_j)$ | direct exchange factor between surface ring element $i$ and gas/volume ring element $j$ |
| $\overline{dss}(\mathbf{r}_i, \mathbf{r}_j)$ | direct exchange factor between surface ring elements $i$ and $j$ |
| $dx$ | axial thickness of gas/volume ring element |
| $E$ | emissive power |
| $h$ | heat transfer coefficient |
| $i$ | enthalpy |
| $\mathbf{I}$ | identity matrix |
| $K_t$ | extinction coefficient |
| $Pr$ | Prandtl number |
| $q$ | radiative heat rate |
| $r$ | radial coordinate |
| $\mathbf{r}$ | position vector |
| $w$ | numerical integration weight factor |
| $x$ | axial coordinate |

**Greek Symbols**

| | |
|---|---|
| $\theta$ | tilt angle of surface with respect to $x$-axis |
| $\psi$ | azimuth angle |
| $\tau$ | transmittance |

**Subscripts**

| | |
|---|---|
| $0$ | stagnation |
| $A$ | adiabatic |
| $i$ | emitting ring element |
| $j$ | receiving ring element |
| $max$ | maximum |
| $min$ | minimum |
| $n$ | station |
| $r$ | radiation |
| $s$ | surface |
| $S$ | static |
| $g$ | gas/volume |
| $G$ | gas |
| $W$ | wall |
| $x$ | reference |


Copyright © 2002 by ASME

## INTRODUCTION

Thermal analysis is an essential and integral part of the design of rocket engines. The need for thermal analysis is especially important in reusable engines where an effective and efficient cooling system is crucial in expanding the engine's life. The rapid and accurate estimation of propulsion system aero-thermodynamic heat loads and thermal protection system effectiveness is required if new vehicle propulsion concepts are to be evaluated in a timely and cost effective manner. In high-pressure engines, hot-gas temperatures can be very high (it can reach 7000°R at the throat area). It is therefore essential to be able to estimate the wall temperature and ensure that the material can withstand such high temperatures. Furthermore, an accurate thermal model enables an engine designer to modify the cooling channel configuration for optimum cooling at high temperature areas. It should be noted that the under-cooling of an engine would result in its catastrophic failure and over-cooling would cause loss of engine performance. This performance loss can be due to the need for a bigger coolant compressor or to decreased effective flow area at the throat when the liner temperature is very low (larger boundary layer displacement when the liner is over-cooled).

The thermal phenomena in rocket engines involve interactions among a number of processes, including: combustion in the thrust chamber; expansion of hot-gases through the nozzle; heat transfer from hot-gases to the nozzle wall via convection and radiation; conduction in the wall; and convection to the cooling channel. The complexity of the thermal analysis in rocket engines is due to: three-dimensional geometry; coolant and hot gas heat transfer coefficient dependence on the pressure and wall temperature; unknown coolant pressure drop and properties; axial conduction of heat within the wall; and radiative heat transfer between gases and surfaces of the engine. A comprehensive thermal model must account for all of these items.

The most commonly used hot-gas model for chemical propulsion systems (TDK, Two Dimensional Kinetics Nozzle Performance Computer Program), Nickerson et al, (1989), considers only convection heat transfer to the wall in evaluating heat flux from combustion gases. In fact, most thermal models neglect the effect of radiation heat transfer even when the propellant is a hydrocarbon fuel, such as RP1. The work presented by Hammad and Naraghi (1991) shows that radiative heat transfer can be up to 30% of total heat transfer from combustion gases to the nozzle wall. They, however, used a one-dimensional model and did not conjugate gas radiation with wall conduction and coolant convection. Liu and Tiwari (1996) studied the effects of radiative heat transfer in chemically reacting nozzle flows. They concluded that for large nozzles, the radiative heat transfer is dominant over the convective wall fluxes. Most recently, Badinand and Fransson (2002) studied radiative heat transfer in film cooled $LH_2/LO_2$ rocket engines . Their results show that the radiation effect would raise the wall temperature of the nozzle by approximately 140K for a shocked nozzle.

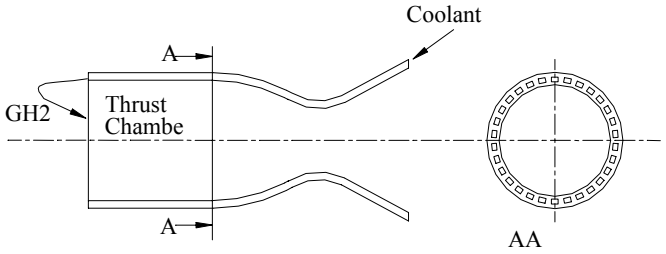


**Figure 1: A typical regeneratively cooled rocket engine**

In this paper a conjugated radiative/conductive/convective model for thermal analysis of regeneratively cooled rockets is used to study the effect of radiation heat transfer on the rocket thermal characteristics, including, coolant temperature, pressure and Mach number. The radiation model is based on the Discrete Exchange Factor (DEF) method for axisymmetric configurations given in Nunes et al., (1998, 2000 and 2001), which incorporates all geometric complications of rocket nozzles (e.g., blockage and shadowing effects due to the throat area). The blockage due to the throat is modeled based on the formulation presented by Modest (1988). Two engines were analyzed in this work: first, a high-pressure chamber with $LH_2$-$LO_2$ (liquid hydrogen and liquid oxygen) propellant and $LH_2$ as the coolant; and second, a high-pressure chamber with RP1-$LO_2$ ($C_{12}H_{23}$ and Liquid Oxygen) propellant and $LO_2$ as the coolant.

## DESCRIPTION OF REGENERATIVELY-COOLED ROCKET ENGINES

A typical regeneratively cooled rocket engine consists of a thrust chamber and a converging-diverging nozzle as shown in Figure 1. To cool the walls of these engines, cryogenic fuel (e.g., liquid hydrogen, RP1, liquid methane) or cryogenic oxidizer (liquid oxygen) is passed through cooling channels that are machined in the wall. Figure 2 shows details of the wall construction, which includes three layers: a coating, channel, and close up. The channel area material is made of a high-conductivity material such as copper alloy. A detailed description of regeneratively cooled rocket engines is given by Huzel and Huang, (1992).

A typical cooling channel has a high aspect ratio in order to maximize heat transfer from the sidewall of the cooling channels. The major issue in designing the cooling system of these engines is in determining the right cooling channel width and height, such that the wall temperature does not exceed the material's thermal limit and the wall temperature does not get too cold to result in loss of engine performance.

For accurately estimating wall temperature, all thermal transport processes in the engine must be conjugated. These processes involve convection and radiation from hot gases, conduction within the wall, and convection to the cooling channel. All these processes are nonlinear and conjugating them requires development of a unique numerical marching technique. This numerical model is outlined in the next section.


Copyright © 2002 by ASME

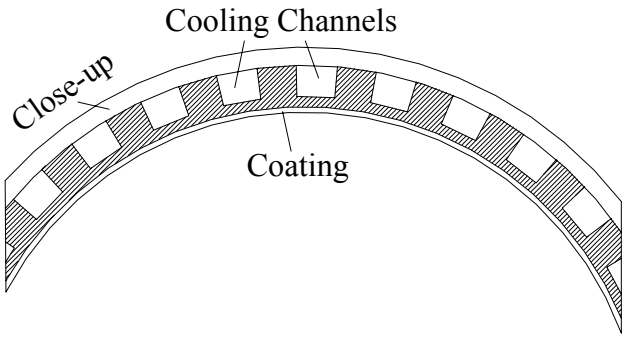


**Figure 2: Detailed layout of cooling channels in a typical regeneratively cooled rocket engine**

## NUMERICAL MODEL

In this model, the rocket thrust chamber and nozzle are subdivided into a number of stations along the longitudinal direction, as shown in Figure 3. These stations do not have to be equally spaced; in fact, it is desirable to have more stations near the throat where the heat flux and temperature gradients are largest. The station numbering starts with the inlet to the cooling channels and ends at their exit. Figure 3 shows a counter flow nozzle liner cooling arrangement. There are other cooling arrangements, where the coolant enters at a point in the middle or the end of the nozzle liner, travels parallel to the hot-gas, makes a U-turn at the exit of the nozzle, and returns as a counter flow coolant in different cooling channels. This arrangement is known as "pass-and-half" or "wrapped" flow cooling.

The numerical marching starts with station 1, where coolant enters the cooling channel and the coolant temperature is known. The thermodynamic and transport properties of the combustion gases are evaluated using the chemical equilibrium composition computer program developed by Gordon and McBride (1971 and 1984) (CET, Chemical Equilibrium with Transport properties). The GASP (GAS Properties), Hendricks et al. (1975) or WASP (Water And Steam Properties), Hendricks et al., (1973) programs are implemented to obtain coolant thermodynamic and transport properties.

Since the wall temperature is unknown for the first march, the adiabatic wall temperature correlations for fast moving nozzle flow presented by Eckert (1972) and Bartz (1965) were implemented to estimate the convective, as well as radiative heat fluxes from the hot-gases. These correlations are:

$$i_{GX_n} = 0.5(i_{GW_n} + i_{GS_n}) + 0.180(i_{G0_n} - i_{GS_n}) \qquad (1)$$

and

$$i_{GAW_n} = i_{GS_n} + (\mathrm{Pr}_{GX_n})^{1/3}(i_{G0_n} - i_{GS_n}) \qquad (2)$$

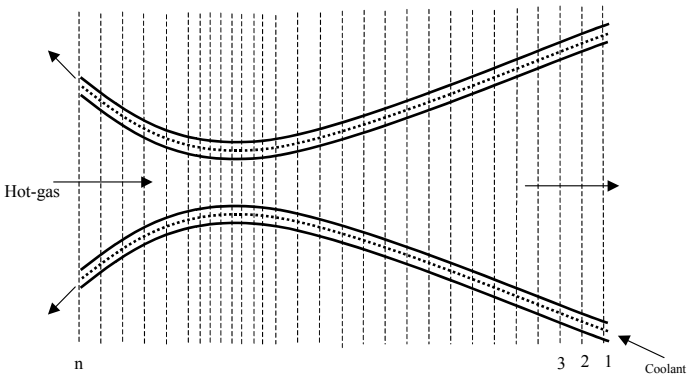


**Figure 3: A rocket nozzle subdivided into a number of stations**

The Dittus-Bolter correlation is used for the first march to evaluate the heat transfer coefficient for the hot-gas-side. The convective wall heat flux is evaluated using

$$q_n = \frac{h_{G_n}}{C_{p_{GX_n}}}(i_{GAW_n} - i_{GW_n}) \qquad (3)$$

It should be noted that since the wall temperature is not known for the first march, the radiation effect is ignored. For the second and subsequent marches, a boundary layer model is used which incorporates a damping factor for accurately predicting the reduced heat transfer rates associated with increased viscous sublayer thickness, or for complete boundary layer laminarization for an accelerating flow. Details of this boundary layer model are discussed by Delise and Naraghi (1994) and Naraghi and Delise (1995).

The radiative heat flux, $q''_r$, which is evaluated for the second and all subsequent marches, consists of radiative heat transfer from the hot-gases and surface of the nozzle. It should be noted that the combustion gas absorption coefficients are spectral and vary along the engine, due to the change in gas composition, temperature and pressure. Edwards' wide band model (Edwards, 1973, 1976) is used to determine spectral absorption coefficients of the gases. Bands for non-homogenous absorption coefficients at various stations do not coincide (due to temperature, pressure and gas composition variation). Hence, a Sum-of-Gray-Gases model was used with weights equal to the integration of the Planck's distribution over each band (Hottel and Sarofim, 1976).

The Discrete Exchange Factor (DEF) method is used to evaluate the radiative heat transfer component of this problem. Radiative exchange among surfaces and/or volumes can be expressed in terms of discrete exchange factors. For arbitrarily-shaped axisymmetric systems, such as the nozzle shown in Figure 4, the DEF equations for radiative transport within an enclosure with varying properties are:


Copyright © 2002 by ASME

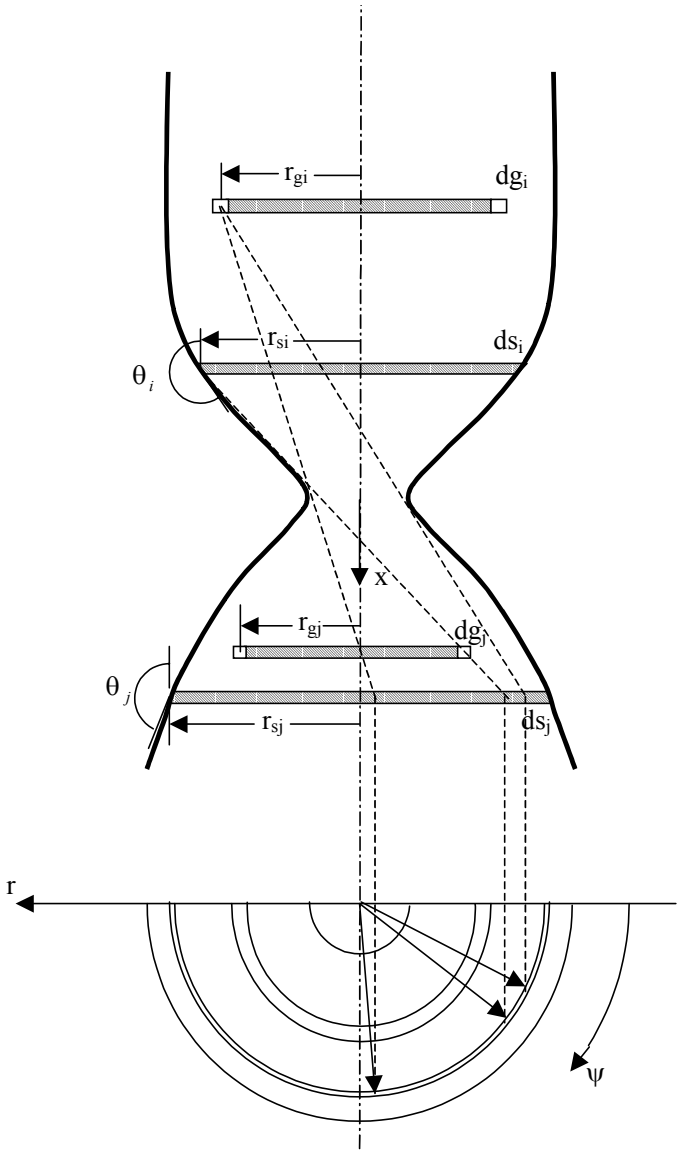


**Figure 4: Configuration of surface and gas/volume ring elements within a nozzle and thrust chamber with throat blockage (shadowing)**

$$\overline{dss}(\mathbf{r}_i,\mathbf{r}_j)=\frac{2r_i r_j^2\cos\theta_i\cos\theta_j ds_j}{\pi}\times\ldots \int_{\psi_{\min}}^{\psi_{\max}}\frac{(\phi_i-\cos\psi)(\phi_j-\cos\psi)\tau(\mathbf{r}_i-\mathbf{r}_j)}{\left|\mathbf{r}_i-\mathbf{r}_j\right|^4}d\psi_j \quad (4)$$

$$\overline{dsg}(\mathbf{r}_i,\mathbf{r}_j)=\frac{-2K_{t_j}r_j^2\cos\theta_i dr_j dx_j}{\pi}\times\ldots \int_{\psi_{\min}}^{\psi_{\max}}\frac{(\phi_i-\cos\psi)\tau(\mathbf{r}_i-\mathbf{r}_j)}{\left|\mathbf{r}_i-\mathbf{r}_j\right|^3}d\psi_j \quad (5)$$

$$\overline{dgs}(\mathbf{r}_i,\mathbf{r}_j)=\frac{-r_i r_j\cos\theta_j ds_j}{2\pi}\times\ldots \int_{\psi_{\min}}^{\psi_{\max}}\frac{(\phi_j-\cos\psi)\tau(\mathbf{r}_i-\mathbf{r}_j)}{\left|\mathbf{r}_i-\mathbf{r}_j\right|^3}d\psi_j \quad (6)$$

$$\overline{dgg}(\mathbf{r}_i,\mathbf{r}_j)=\frac{K_{t_j}r_j dr_j dx_j}{2\pi}\int_{\psi_{\min}}^{\psi_{\max}}\frac{\tau(\mathbf{r}_i-\mathbf{r}_j)}{\left|\mathbf{r}_i-\mathbf{r}_j\right|^2}d\psi_j \quad (7)$$

where

$$\phi_i=\frac{r_i}{r_j}+\frac{z_j-z_i}{r_j}\tan\theta_i \quad (8)$$

and

$$\phi_j=\frac{r_j}{r_i}+\frac{z_i-z_j}{r_i}\tan\theta_j \quad (9)$$

The transmittance, $\tau$, in the DEF equations can be defined as:

$$\tau(\mathbf{r}_i-\mathbf{r}_j)=e^{-\int_{r_i}^{r_j}K_t(\mathbf{r})d\mathbf{r}} \quad (10)$$

The hot-gases in the thrust chamber and nozzle form a non-homogenous medium (composition, pressure and temperature of hot-gases change with axial position); hence the extinction coefficient changes with position. The limits of integration in equations (4-7) are $\psi_{\min}$ and $\psi_{\max}$ and these are the minimum and maximum azimuth angles at which ring element *j* is seen from a point on ring element *i*. The allowable range of $\psi$ is dictated by the orientation and relative position of the ring position of each ring element pair. It is possible that, in many instances, the view between ring element pairs is partially obstructed by the throat. The blockage angle, $\cos^{-1}\Gamma$, is evaluated by projecting a line from a point on an emitting ring element (denoted by *i*) around the periphery of the blocking body at an axial position $x_k$, such that $x_k$ is between $x_i$ and $x_j$.


Copyright © 2002 by ASME

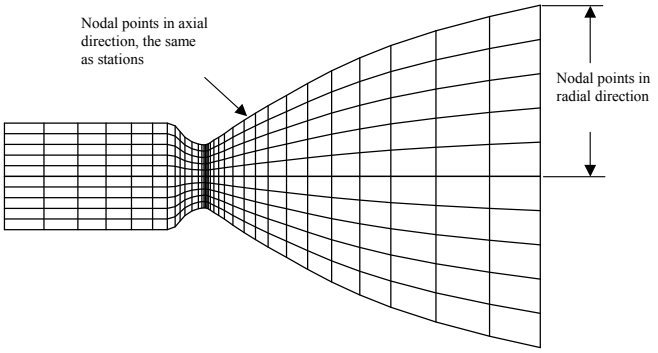


**Figure 5: Position of surface nodes and gas nodes for the radiation model**

The intersection point between the receiving ring element (denoted by *j*) and the shadowing produced by the blocking body at $x_k$ results in a minimum azimuth angle. This procedure is repeated for several values of $x_k$ and can mathematically stated as:

$$\Gamma = \min\left(\frac{A-B-C}{D}\right)_{x_k \in (x_i, x_j)} \tag{11}$$

where

$$A = \left[D_G(x_k)/2\right]^2 (x_j - x_i)^2;\ B = r_i^{\,2}(x_j - x_k)^2$$
$$C = r_j^{\,2}(x_k - x_i)^2;\ D = 2r_i r_j (z_k - z_i)(z_j - z_k) \tag{12}$$

The minimum and maximum azimuth angles can then be calculated from:

$$\psi_{\min} = \cos^{-1}[\min(\phi_i, \phi_j, \Gamma, 1)];\quad \psi_{\max} = \pi \tag{13}$$

The direct exchange factors calculated based on the above formulation accuount for direct exchange of radiation between surface and gas elements. To account for multiple reflections and scattering of radiation, total exchange factors are computed. The total exchange factor between two elements is defined as the fraction of the radiative energy that is emitted from one element and absorbed by the other element via direct radiation and multiple reflections from surfaces, as well as scattering within the gas. The total exchange factor expressions are:

$$\overline{\mathbf{DSS}} = \left[\mathbf{I} - \left\{\overline{\mathbf{dss}} + \overline{\mathbf{dsg}}\omega_0 \mathbf{W_g}\left[\mathbf{I} - \overline{\mathbf{dgg}}\omega_0 \mathbf{W_g}\right]^{-1}\overline{\mathbf{dgs}}\right\}\boldsymbol{\rho}\mathbf{W_s}\right]^{-1} \cdot \left\{\overline{\mathbf{dss}} + \overline{\mathbf{dsg}}\omega_0 \mathbf{W_g}\left[\mathbf{I} - \overline{\mathbf{dss}}\omega_0 \mathbf{W_g}\right]^{-1}\overline{\mathbf{dgs}}\right\}\boldsymbol{\alpha} \tag{14}$$

$$\overline{\mathbf{DGS}} = \left[\mathbf{I} - \overline{\mathbf{dgg}}\omega_0 \mathbf{W_g}\right]^{-1}\overline{\mathbf{dgs}} \cdot \left[\mathbf{I} - \boldsymbol{\rho}\mathbf{W_s}\left\{\overline{\mathbf{dss}} + \overline{\mathbf{dsg}}\omega_0 \mathbf{W_g}\left[\mathbf{I} - \overline{\mathbf{dgg}}\omega_0 \mathbf{W_g}\right]^{-1}\overline{\mathbf{dgs}}\right\}\right]^{-1}\boldsymbol{\alpha} \tag{15}$$

where $\overline{\mathbf{DSS}} = \left[\overline{DS_i S_j}\right]$, $\overline{\mathbf{DVS}} = \left[\overline{DV_i S_j}\right]$ are matrices representing total exchange factors from surface and gas axisymmetric rings to surface elements; $\overline{\mathbf{dss}} = \left[\overline{ds_i s_j}\right]$, $\overline{\mathbf{dsg}} = \left[\overline{ds_i g_j}\right]$, $\overline{\mathbf{dgs}} = \left[\overline{dg_i s_j}\right]$, $\overline{\mathbf{dgg}} = \left[\overline{dg_i g_j}\right]$ are matrices for direct exchange factors between surface/volume ring elements; $\mathbf{W_s} = \left[w_{s,i}\delta_{i,j}\right]$ and $\mathbf{W_g} = \left[w_{g,i}\delta_{i,j}\right]$ are diagonal matrices for numerical integration weight factors for surface/volume ring elements, respectively; and $\rho = \left[\rho\delta_{i,j}\right]$ and $\alpha = \left[\alpha\delta_{i,j}\right]$ are diagonal matrices of reflectivities and absoptivities for surface ring elements.

Once the total exchange factors are evaluated using equations (14) and (15), the radiative heat flux at the *n*-th station is computed using the following energy balance equation:

$$q_{r,n} = \sum_{j=1}^{2n_r+m} w_{s,j}\,\overline{DS_j S_n}E_{s,j} + \sum_{j=1}^{m\cdot n_r} w_{g,j}\,\overline{DG_j S_n}E_{g,j} - E_{s,n} \tag{16}$$

where $E_{s_n}$ and $E_{g_n}$ are surface and gas emissive powers at station *n*. Note that the first term in the right-hand-side of equation (16) is the incident radiative flux at the surface due to emission from other surface elements, the second term is due to the radiative flux from gas elements, and the last term is the radiative heat loss due to emission.

The present model has been benchmarked against a number of known exact solutions and solutions that are available for a number of cylindrical problems. The results reported by Nunes et al. (1998, 2000 and 2001) show excellent agreement between the results of this model and published data.

Before performing axial marches, the radiation model evaluates total exchange factors based on the Discrete Exchange Factor (DEF) method. In this model, the nozzle is subdivided into a number of volume and surface nodes as shown in Figure 5. The number of radial nodes is set to 5. The number of axial nodes is the same as the number of stations. The position of axial nodes coincide with those of the stations. Since the exchange factors are dependent on gas and surface radiative properties and the geometry of the nozzle, they are calculated first. Since the composition of combustion gases varies with axial position, radiative properties of combustion gases are not constant (the gases are non-homogenous).

The wall temperature distribution is evaluated using a three-dimensional model. This model has been specifically


Copyright © 2002 by ASME

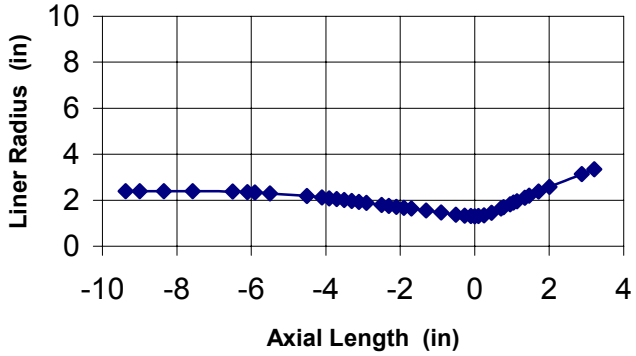


**Figure 6: The LH2-LO2 rocket thrust chamber contour showing station locations**

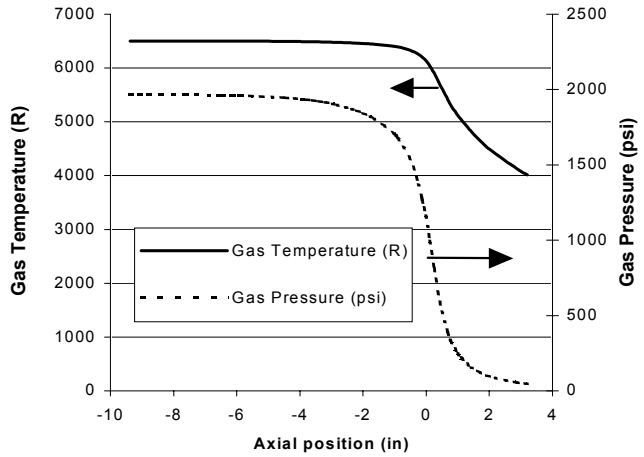


**Figure 7: Gas temperature and pressure along the axial direction for the LH2-LO2 engine for a chemical equilibrium condition**

developed for three-dimensional conduction in rocket thrust chambers and nozzles, as shown in Figure 1. Because of the symmetry of the configuration, computations are performed for only one cell (half cooling channel and half land). A two-dimensional finite difference grid is superimposed on cells at all stations. The energy balance equation for each node is based on the exchange of heat between neighboring nodes at the same station, and at two neighboring stations (i.e., stations n+1 and n-1).

The coolant flow is formulated based on a one-dimensional model, which incorporates supercritical coolant properties, pressure drop, expansion and contraction of cooling channels and curvature effects; The coolant heat fluxes are evaluated based on correlations specifically developed for each coolant. For example, for supercritical liquid hydrogen the correlation suggested by Hendricks et al. (1985), and for liquid oxygen the correlation developed by Spencer and Rouser (1977), are used. A complete description of the numerical model for this Rocket Thermal Evaluation model is posted at www.manhattan.edu/~mnaraghi/rte/rte.html.

## RESULTS AND DISCUSSION

In order to show the effects of radiation heat transfer on the wall temperature and on the coolant flow of typical regeneratively cooled rocket thrust chambers and nozzles, two cases, with commonly used propellants and coolants, were evaluated. The first case is for a high-pressure chamber design with liquid hydrogen and liquid oxygen ($LH_2$-$LO_2$) as the propellant. The second case is for a high-pressure chamber design with RP1 (a hydrocarbon propellant) and liquid oxygen as an oxidizer and coolant (RP1-$LO_2$).

### $LH_2$-$LO_2$ Chamber

The specifications of this engine are:

| | |
|---|---|
| Chamber pressure | 2000 psia |
| O/F | 5.8 |
| Contraction ratio | 3.41 |
| Expansion ratio | 6.63 |
| Throat diameter | 2.6 inches |
| Propellant | $LH_2$-$LO_2$ |
| Coolant | LH2 |
| Total coolant flow rate | 6.45 lb/s |
| Coolant inlet temperature | $50^oR$ |
| Coolant inlet stagnation pressure | 2900 psia |
| Throat region channel aspect ratio | 6 |
| Number of cooling channels | 150 |

The contour of this rocket thrust chamber and nozzle is shown in Figure 6, with the station locations denoted on the contour. A total of 41 stations were considered in analyzing this engine. The rocket thermal analysis model is used to generate results with and without radiation. Figure 7 shows the results for propellant temperature and pressure distributions evaluated on the basis of the Rocket Performance module of the Chemical Equilibrium code (Gordon and Mcbride, 1971). The same code provides the composition and mole fraction of species in the combustion gases. The gas is assumed non-homogenous (absorption coefficient of the gas varies with gas composition, temperature and pressure along the axial direction) and Edwards' (1972, 1976) wide band model was used to obtain spectral properties of combustion gases. For this engine, $H_2O$ is the only species that has a significant thermal radiation absorption coefficient. The mole fraction of $H_2O$ varies from 60% to 74% for the combustion gases. The Weighted-Sum-of-Gray-Gases model was then used to obtain a single value for the gas absorption coefficient at each station with the weights being the integration of Planck's distribution (black body emission) over each band.

Figure 8 shows the resulting wall heat flux distribution. As shown, the effect of radiation is negligible for the diverging section of the engine. This low radiative flux effect is due to the


Copyright © 2002 by ASME

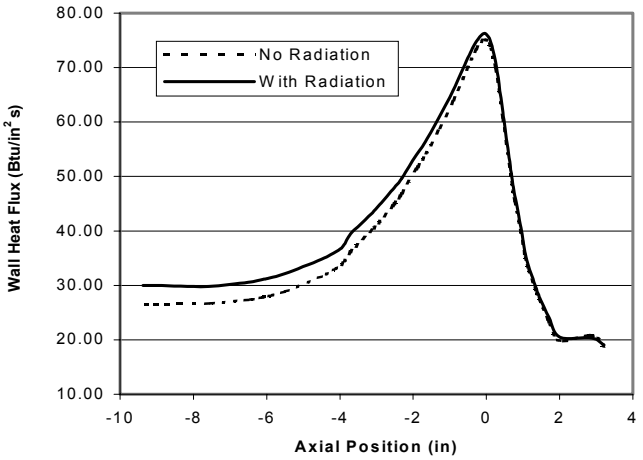


**Figure 8: Effects of radiation on the wall heat flux at different axial location for the LH2-LO2 engine**

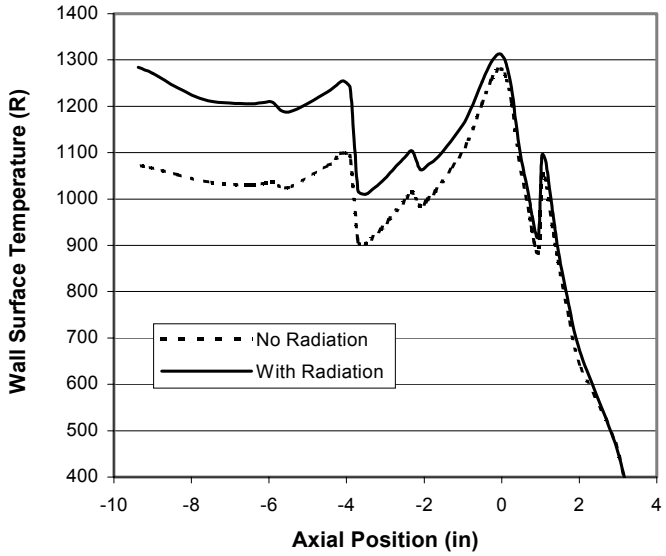


**Figure 9: Effects of radiation on the wall temperatures of the LH2-LO2 engine**

low surface/gas emission (low gas temperature and emissivity in the diverging section of the nozzle) to low temperature gases at the exit of the nozzle. The effect of radiative heat flux is more pronounced in the converging section of the nozzle and the thrust chamber where the gas temperature and gas emissivity are large. The results indicate that the radiation heat flux can reach 10% of the overall wall heat flux in the thrust chamber. This increase in wall heat flux due to radiation, although small, can have a significant effect on the wall temperature. Figure 9 shows the wall surface temperature distribution for both no radiation and radiation. As expected, the effect of radiation on the wall temperature is negligibly small for the diverging section of the engine.

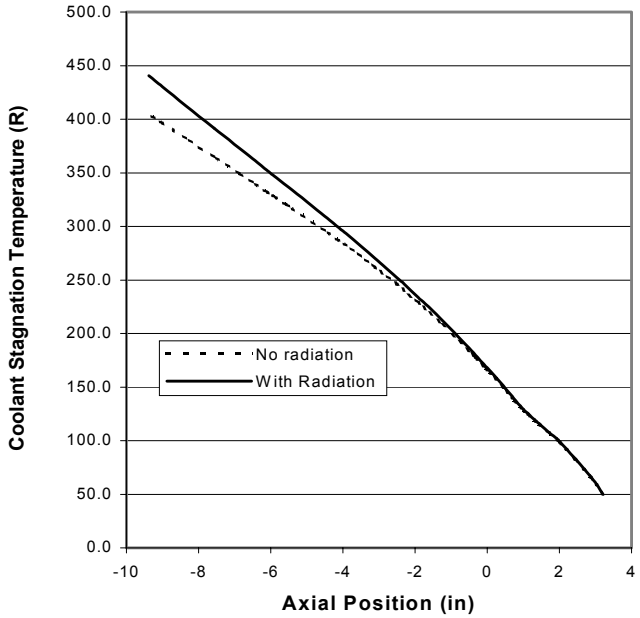


**Figure 10: Effects of radiation on the coolant stagnation temperature versus axial position for the LH2-LO2 engine**

This figure shows that the peak temperature occurs at the throat area (axial position 0). There are also some local peak temperature points, which are caused by step changes in cooling channel width or height. These local peak temperatures are smaller than the throat temperature when radiation is neglected. As shown in Figure 9, the effect of radiative flux results in a substantial increase of the local peak temperatures, such that they come close to the maximum temperature (throat temperature). The figure also shows that the difference between wall temperatures for the no-radiation and radiation cases is larger toward the left side of the graph (larger downstream of the cooling channel). This is due to the fact that additional radiative heat picked up by the coolant results in a higher coolant temperature, and hence larger wall temperatures in the thrust chamber. Figure 10 shows the increased stagnation temperature of the coolant due to the radiation heat flux.

**RP1-$LO_2$ Chamber**

The specifications of this engine are:

| | |
|---|---|
| Chamber pressure | 2400 psia |
| O/F (mixture ratio) | 2.8 |
| Contraction ratio | 3.97 |
| Expansion ratio | 46.96 |
| Throat diameter | 1.255 inches |
| Propellant | RP1-$LO_2$ ($C_{13}H_{23}$-$LO_2$) |
| Coolant | $LO_2$ |
| Total coolant flow rate | 11.94 lb/s |
| Coolant inlet temperature | 150$^o$R |
| Coolant inlet pressure | 4100 psi |
| Throat region channel aspect ratio | 6 |


Copyright © 2002 by ASME

| | |
|---|---|
| Number of cooling channels | 100 (diverging section)<br>200 (chamber, converging section and throat) |

Figure 11 shows the contour of this thrust chamber and nozzle, with stations denoted on the contour. A total of 37 stations were considered in analyzing this engine. The gas static temperature and pressure for this engine were evaluated based on the chemical equilibrium conditions, and is shown in Figure 12. The species in the combustion gases that contribute to the absorption and emission of radiation for this engine are: $H_2O$, $CO_2$ and CO. Their mole fractions vary across the chamber and nozzle, however the average percentages of their mole fractions are: 33% $H_2O$, 17% $CO_2$ and 30% CO. Similar to the previous case, the gas absorption coefficients, based on the gas composition, pressure, temperature and optical length, are determined using the Edwards wide band and Sum-of-Gray-Gases models.

Similar to the $LH_2$-$LO_2$ engine, the resulting wall heat flux profile (see Figure 13) shows almost no difference at the diverging section of the engine between the no-radiation and radiation cases. The difference between the two heat fluxes is, however, much larger in the thrust chamber and converging section of the engine. The resulting wall surface temperature distributions for the no-radiation and radiation cases are shown in Figure 14. These results demonstrate that there is about a 3 to 4 percent increase in the wall temperature due to radiation in the diverging section of the nozzle (positive axial position) and the throat area. For the converging section, however, the effect of radiation results in a substantial increase in wall temperature (more the 20%).

A major issue in designing cooling channels of regeneratively cooled rocket engines is to ensure that the coolant pressure at the exit of the cooling channel is adequate for the injector. For the first engine, the increased heat flux due to radiation did not make a significant change in the coolant pressure. For the present engine, however, as shown in Figure 15, the increase in heat flux due to radiation causes a significant change in coolant pressure at the exit of the cooling channel (about 450 psi). One reason for such a large pressure drop can be due to the poor cooling characteristics of LO2. The results for coolant temperature show a 15% increase in coolant stagnation temperature (see Figure 16).

Another coolant characteristic that should be watched closely is the coolant Mach number. Generally, the coolant Mach number is kept below 0.35 through the cooling passage. The results of Figure 17 show that the coolant Mach number is in fact less than 0.35 throughout the engine when the effect of radiation is neglected. The results with radiation, however, show that the coolant Mach number exceeds this critical value at the throat area, and at the exit of cooling channel.

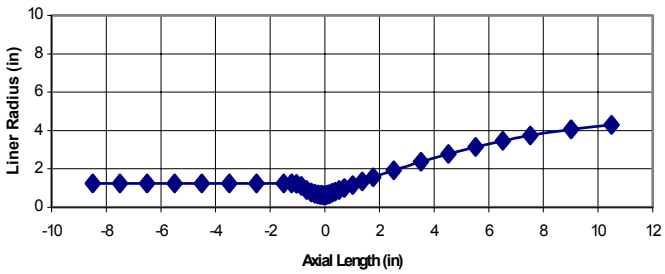


**Figure 11: RP1-LO2 rocket thrust chamber and nozzle contour showing station locations**

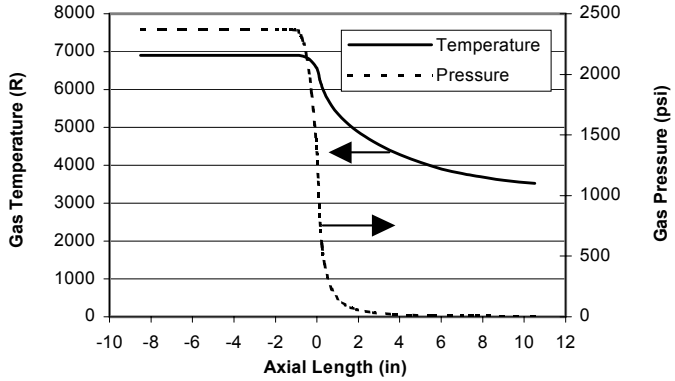


**Figure 12: RP1-LO2 gas static temperature and pressure at different locations in the thrust chamber and nozzle, for a chemical equilibrium condition**

## CONCLUDING REMARKS

The effects of gas and surface radiation on the wall temperature, coolant pressure/temperature and Mach number were studied. The results presented demonstrate that although the increase in heat flux due to radiation is small, it can have a significant effect on the wall temperature and coolant flow characteristics.

For an LH2/LO2 engine it is shown that the radiation has a small effect on the wall temperature of the diverging section of the nozzle. However, the radiation results in a substantial increase in the wall temperature of the thrust chamber and converging section of the nozzle, such that the local peak temperature is the same order of magnitude as the throat temperature.

For the RP1-LO2 engine, radiation heat transfer resulted in an increase in wall temperature of 20%. Additionally, it significantly increased the coolant pressure drop and Mach number, indicating that neglecting radiation during design may result in a faulty cooling system.


Copyright © 2002 by ASME

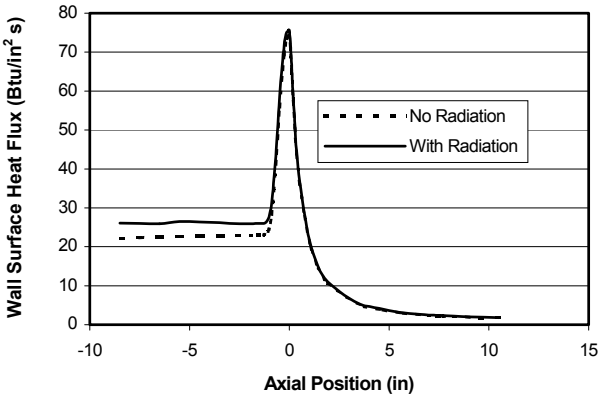


**Figure 13: Effect of radiation on the wall heat flux of a LO2 cooled RP1-LO2 engine**

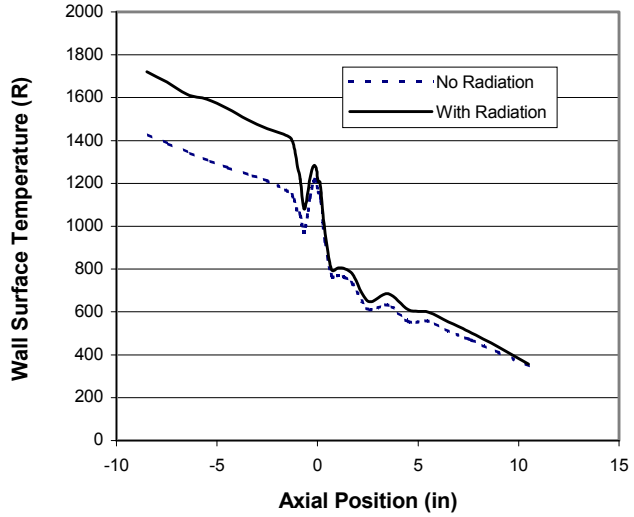


**Figure 14: Effects of radiation on the wall temperature of a LO2 cooled RP1-LO2 engine**

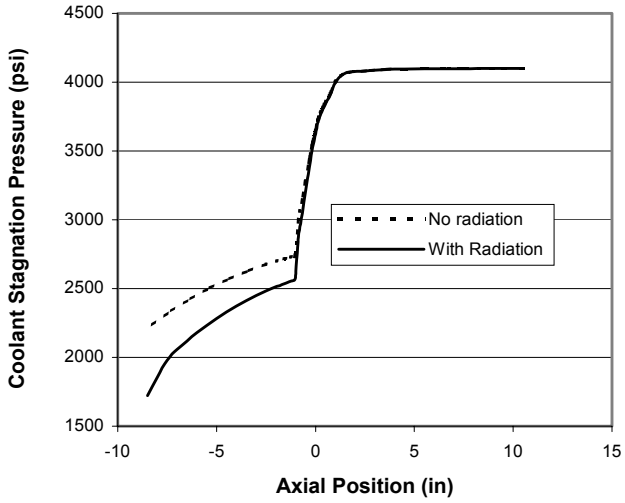


**Figure 15: Effect of radiation on coolant pressure of a LO2 cooled RP1-LO2 engine**

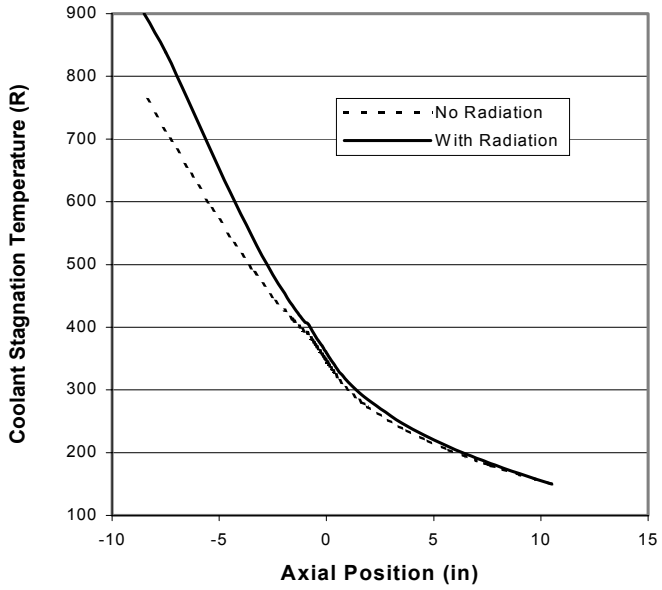


**Figure 16: Effect of radiation on the coolant stagnation temperature of a LO2 cooled RP1-LO2 engine**

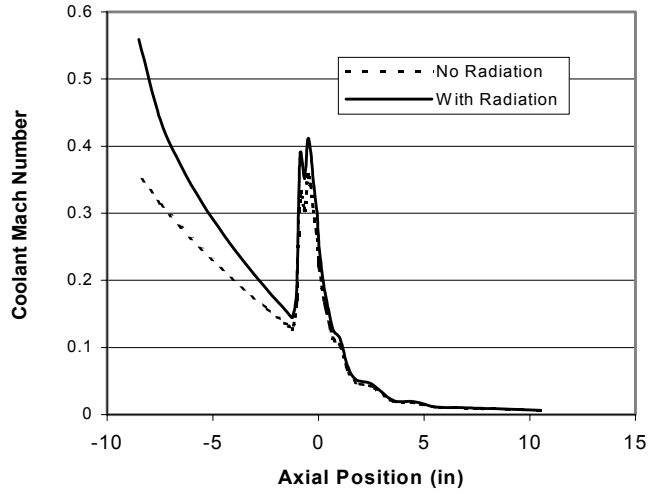


**Figure 17: Effect of radiation on the coolant Mach number of a LO2 cooled RP1-LO2 engine**

## REFERENCES

Badinand, T. and Fransson, T.H., 2002, "Study of Radiative Heat Transfer in Film Cooled LH/LO Rocket Engine Thrust Chamber, Presented at the 2002, Aerospace Science Conference, Reno, Nevada.

Bartz, D. R., 1965, "Turbulent Boundary-Layer Heat Transfer from Rapidly Accelerating Flow of Rocket Combustion Gases and of Heated Air," Advances in Heat Transfer, pp. 2-108, 1965.


Copyright © 2002 by ASME

DeLise, J. C., and Naraghi, 1995, “A Comparative Study of Boundary Layer Models for Converging Diverging Nozzles”, AIAA paper 95-2499, presented at the 31st AIAA/ASME/SAE/ASEE Joint Propulsion Conference and Exhibit, San Diego, CA, July 10-12.

Eckert, E. R. G. and Drake, R. M., 1972, *Analysis of Heat and Mass Transfer*, McGraw-Hill Book Company.

Edwards, D.K., and Balakrishnan, 1972, “Slab Band Absorptance for Molecular gas Radiation,” Journal of Quant. Spectrosc. Radiant. Transfer, Vol. 12, pp. 1379-1387.

Edwards, D.K., 1976, “Molecular Gas band Radiation,” Advances in Heat Transfer, Vol. 12, pp. 115-193, Editors: T.F. Irvine and J.P. Hartnett, Academic Press, New York.

Gordon, S. and McBride, B. J., 1971, “Computer Program for Calculation of complex Chemical Equilibrium Compositions, Rocket Performance, Incident and Reflection Shocks, and Chapman-Jouquet Detonations,” NASA SP-270.

Gordon, S., McBride, B. J. and Zeleznik, F. J., 1984,“Computer Program for Calculation of Complex Chemical Equilibrium Compositions and Applications Supplement I - Transport Properties,” NASA TM-86885.

Hammad, K.J., and Naraghi, M.H.N., 1991 “Exchange Factor Model for Radiative Heat Transfer Analysis in Rocket Engines,” AIAA Journal of Thermophysics and Heat Transfer, Vol. 5, No. 3, pp. 327-334.

Hendricks, R. C., Baron, A. K. and Peller, I. C., “GASP - A Computer Code for Calculating the Thermodynamic and Transport Properties for Ten Fluids: Parahydrogen, Helium, Neon, Methane, Nitrogen, Carbon Monoxide, Oxygen, Fluorine, Argon, and Carbon Dioxide,” NASA TN D-7808, Feb. 1975.

Hendricks, R. C., Peller, I. C. and Baron, A. K., “WASP - A Flexible Fortran IV Computer Code for Calculating Water and Steam Properties,” NASA TN D-7391, Nov, 1973.

Hendricks, R. C., Niino, M., Kumakawa, A., Yernshenko, V. M., Yaski, L. A., Majumdar, L. A., and Mukerjee, J., “Friction Factors and Heat Transfer Coefficients for Hydrogen Systems Operating at Supercritical Pressures,” Proceeding of Beijing International Symposium on Hydrogen Systems, Beijing, China, May 7-11, 1985.

Hottel, H.C., and Sarofim, A.F., *Radiative Transfer*, McGraw-Hill, New York, 1967.

Huzel, D. K., and Huang, D.H., 1992*, Modern Engineering for Design of Liquid-Propellant Rocket Engines*, Progress in Astronautics and Aeronautics, Vol. 147, AIAA.

Liu, J., and Tiwari, S.N., 1996, “Radiative Heat Transfer Effects in Chemically Reacting Nozzle Flows,” Journal of Thermophysics and Heat Transfer, Vol. 10, No. 3, 1996.

Modest, M.F., 1988, “Radiative Shape Factors Between Differential Ring Elements on Concentric Axisymmetric Bodies,” Journal of Thermophysics and Heat Transfer, Vol. 2, No. 1, pp. 86-88.

Nickerson, G.R., Coats, D.E., Dang, A.L., Dunn, S.S., and Kehtarnavaz, H., 1898, *Two-Dimensional Kinetics (TDK) Nozzle Performance Computer Program*, NAS8-36863.

Naraghi, M.H.N., and DeLise, J.C., 1995, “Conjugate Conductive, Convective and Radiative Heat Transfer in Rocket Engines,” ASME publication HTD-Vol 307, 1995 National Heat Transfer Conference –Volume 5, pp. 65-79.

Nunes, E.M., Naraghi, M.H.N., and Modi, V., 2001, “Radiative Transfer in Axisymmetric Bodies With Non-homogenous Media,” presented at the 35th National Heat Transfer Conference, Anaheim California, June 10-12.

Nunes, E.M., Modi, V., and Naraghi, M.H.N., 2000,"Radiative Transfer in Arbitrarily-Shaped Axisymmetric Bodies with Anisotropic Scattering Media," International Journal of Heat and Mass Transfer, Vol. 43, pp. 3275-3285.

Nunes, E.M., Naraghi, M.H.N., 1998, ``A Model for Radiative Heat Transfer Analysis in Arbitrarily-Shaped Axisymmetric Enclosures", Numerical Heat transfer, Part A, Vol. 33, pp. 495-513.

Spencer, R.G. and Rousar, D.C., 1977, “Supercritical Oxygen Heat Transfer,” NASA CR-135339.

 Copyright © 2002 by ASME